https://doi.org/10.5194/egusphere-2025-2341
Preprint. Discussion started: 5 June 2025

Brief Communication: Decadal changes in topography, surface water and subsurface structure across an Arctic coastal tundra site

Jonathan A. Bachman[1], John Lamb[1], Craig Ulrich[1], Neslihan Taş[1], Baptiste Dafflon[1]
[1]Earth and Environmental Sciences, Lawrence Berkeley National Laboratory, Berkeley, CA, USA
Correspondence to: Baptiste Dafflon (bdafflon@lbl.gov)

Abstract. Understanding changes in water and carbon cycling in permafrost landscapes requires assessing the co-evolution of microtopography, surface water distribution, and subsurface structure. This study evaluates such changes at a coastal Arctic polygonal tundra site by comparing data from two surveys conducted a decade apart. Each survey includes electrical resistivity tomography, active layer thickness, photogrammetry, and topographic data. Results reveal subsidence and permafrost thaw with varying intensity and spatial distribution across polygon types, alongside diverse thermal-hydrological responses, such as thaw pond formation in high-centered-polygons and more even subsidence in flat-centered-polygons. The study also underscores the value and limitations of sporadic surveys.

1 Introduction

The Arctic, which contains a substantial carbon reservoir locked within permafrost soil, is warming nearly four times faster than the global average and experiencing extreme changes in geomorphology, hydrology, and biogeochemistry as ground temperatures cross the 0 °C threshold (Tarnocai et al., 2009). Permafrost thaw can lead to major shifts in topography, water distribution, carbon storage and fluxes, energy balance, vegetation, and erosion rates. The complex feedback mechanisms within and between Arctic ecosystems and atmospheric processes introduce considerable uncertainty into climate projections (Koven et al., 2011).

Field-based assessment of the co-evolution of microtopography, water distribution and subsurface structure across polygonal tundra landscapes is essential to enhance our understanding of how surface and subsurface hydrology and carbon fluxes evolve, yet such investigations remain rare (Abolt et al., 2024; Jorgenson et al., 2006; Streletskiy et al., 2017). The study by Jorgenson et al. (2006) highlights an abrupt increase in permafrost degradation, primarily in massive wedges of ice, on the central Beaufort Coastal Plain in northern Alaska. The area of degrading ice wedges increased from 0.6% in 1982 to 4.4% by 2001. More recently, the work by Abolt et al. (2024) provides insights into thermokarst pool expansion across 27 circumpolar field sites, finding that 44% (±15%) of survey areas experienced pool expansion greater than 3% per year, with an 11% annual increase between 2010 and 2019 at a lowland site near Utqiaġvik (Abolt et al., 2024).

https://doi.org/10.5194/egusphere-2025-2341
Preprint. Discussion started: 5 June 2025

Assessing the co-evolution of permafrost thaw, topography, and water distribution is hindered by the lack of high-resolution and multi-scale observations of terrain and subsurface properties (Dafflon et al., 2016). A particular challenge is the difficulty of quantifying, over space and time, the ice content across the landscape and the associated subsidence driven by ice loss and ground compaction as permafrost thaws (Kokelj & Jorgenson, 2013). Additionally, measurements of ground properties are often referenced to the ground surface – a shifting reference point – introducing uncertainties that are frequently overlooked. For instance, long-term measurements of active layer thickness underestimate the rate of permafrost thaw when subsidence is not accounted for (Rodenhizer et al., 2020; N. I. Shiklomanov et al., 2013; Streletskiy et al., 2017). Rodenhizer et al. (2020) finds that accounting for subsidence increases estimated permafrost thaw by 19–49% and the estimated amount of newly-thawed carbon by 37–113%. Collectively, these studies underscore the importance of jointly assessing potential changes in topography, water distribution, and subsurface structure.

In this brief communication we explore how changes in surface water distribution are associated with changes in topography and permafrost thaw across various polygon types. To this end, we evaluate decadal changes in surface water distribution, thaw layer thickness, terrain elevation, and subsurface structure from the meter to hundreds-of-meters scale over a 12-year period across a polygonal tundra area near Utqiaġvik, Alaska. Besides evaluating the organization of these changes, this study aims to discuss the value and limitations of ground-based methods for sporadic assessment of the evolution of polygonal ground.

1.1 Study Site

The study site, located within the Barrow Environmental Observatory (BEO) on the Alaskan Arctic Coastal Plain, lies approximately 4 miles from the Beaufort Sea near Utqiagvik, Alaska. The landscape is characterized by low topographic relief, with elevations ranging from 2 to 6 meters, and is dominated by polygonal ground formations (Hinkel et al., 2001). The geomorphology of these polygons defines the microtopography, while larger topographical patterns are shaped by processes such as ice accumulation, drainage network evolution, and landscape uplift (Kanevskiy et al., 2017). The polygons are often classified into three categories, high-centered (HCP), flat-center (FCP) and low-centered (LCP) polygons, distinguished by the relative height of their centers compared to the surrounding rims and troughs (Mackay, 2000). High-centered polygons have elevated centers associated with drier conditions, while low-centered polygons exhibit wet centers with well-defined rims and troughs. Flat-centered polygons represent an intermediate form, with flat terrain and wet troughs. These various polygon types, associated with different patterns of water distribution, vegetation cover, and thermal properties, impact carbon fluxes in the Arctic tundra.

Meteorological data shows a warming trend at our field site, with decreasing freezing degree days and increasing thawing degree days from 1991 to 2023 (NOAA Barrow Atmospheric Baseline Observatory, https://gml.noaa.gov/data/data.php?category=Meteorology&site=BRW) (Fig. S1) (Farquharson et al., 2022). Data from the Circumpolar Active Layer Monitoring (CALM) site near Utqiagvik indicate an averaged increase in thaw depth of 0.3 cm/year

https://doi.org/10.5194/egusphere-2025-2341
Preprint. Discussion started: 5 June 2025

for the same period, though inter-annual variability is significant (N. Shiklomanov, 2023) (Fig. S1). In addition, a study evaluating subsidence in the same region over the 2003–15 period reports a subsidence trend of 0.4–1.0 cm/year, resulting in a net elevation change of 8–15 cm over that period (Streletskiy et al., 2017). These datasets indicate the presence of a warming trend and subsequent geomorphological changes in the region.

The permafrost temperature at the study site remains well below 0°C, fluctuating between -12°C and -5°C at a depth of 3 meters, yet the permafrost is not always entirely frozen due to the presence of saline permafrost. Core samples reaching 3 to 6 meters depth around Utqiagvik, AK indicate salinity up to twice that of seawater (Brown, 1969; Dafflon et al., 2016).

The measurements presented in this study were collected in a 475 m long, 20 m wide corridor crossing HCP, FCP and LCP zones (Dafflon et al., 2016). This area was intensively studied between 2011 and 2014 to improve the understanding of the co-variability of microtopography with surface and subsurface properties, the development of zonation approaches to estimating subsurface properties, and the advancement of parameterization and evaluation of terrestrial ecosystem models. A comprehensive examination of the permafrost characteristics in the area indicates that the saline permafrost is spatially continuous, depth-variable, and that the increase in salinity is correlated with a decrease in ice content. The analysis of soil cores collected at this site reveals ice content as high as 85% in the top 1 meter of permafrost and as low as 40% at 2.5 meters depth (Dafflon et al., 2016; Wu et al., 2018). Further, geophysical data indicate that the ice content in the top 2 m is greater in HCP and LCP zones than in FCP area. These results underline the covariability between topography and permafrost characteristics including ice content and salinity distribution. In their study, Dafflon et al. (2016) evaluated terrain elevation using UAV-based photogrammetry, subsurface structure using Electrical Resistivity Tomography (ERT) and soil properties by analyzing soil core and measuring thaw depth. A similar characterization approach is used in this study to evaluate decadal changes in terrain elevation, geomorphology, surface water distribution, and subsurface characteristics.

2 Methods

2.1 Digital Surface Model, Orthomosaic, and Surface Water Distribution

In July 2013, a kite-based aerial system was used to capture high-resolution imagery of the study area (Dafflon et al., 2016). A Sony NEX-5R digital camera was mounted on a Picavet rig positioned approximately 2 meters below the kite line, enabling stable, downward-looking shots from an altitude of about 45 meters. Images were captured automatically at 3-second intervals, covering roughly 73 by 48 meters per frame with a pixel resolution of 0.015 meters. In September 2023, aerial imagery was acquired using a similar methodology, but with a DJI Mini 2 UAV platform. For both surveys (2013 and 2023), ground control targets, spaced approximately 20 meters apart, were positioned along the corridor and surveyed using a centimeter-grade real-time kinematic (RTK) differential GPS system. Agisoft Metashape software was used to extract features, align images, and produce georeferenced outputs, including a digital surface model (DSM) and RGB orthomosaic for each campaign. Analysis of the data products indicated that the DSM can be used as a terrain model proxy because of the low-stature vegetation, and

https://doi.org/10.5194/egusphere-2025-2341
Preprint. Discussion started: 5 June 2025

that the products achieved a spatial resolution of approximately 0.05 m, with positioning accuracy within 6 cm across all axes (x, y, z). The DSM and RGB orthomosaic were used to evaluate changes in water distribution and topography using Python and Matlab. Visualization Toolkit (VTK) and ParaView were used to generate a 3D animation showcasing topography, vegetation, and water distribution in 2013 and 2023 [https://youtu.be/1_5yZp7yw94].

A Random Forest model was applied to the 2013 and 2023 RGB orthomosaics to classify water versus non-water pixels. Given the distinct visual characteristics between the two years –with the 2023 image containing more visible surface water, and the 2013 image showing denser vegetation with underlying water– manual pixel selection for training was required to improve model accuracy. The training dataset consisted of approximately one hundred thousand manually labeled pixels from a subset area of the orthomosaics. Each year's labeled pixels were split into an 80 % training set and a 20 % held out test set. A random forest classifier was then trained on four features, the RGB channels plus the blue to green channel ratio. On the independent test set, the models achieved an accuracy of ~98% for both years. The models were applied to the entire orthomosaics to predict water presence at the pixel level, and the resulting maps were subtracted to visualize surface-water changes.

2.2 Subsurface Properties and Structure

A 475-meter long electrical resistivity tomography (ERT) transect along the centerline of the studied corridor was acquired in September 2011 and 2023 using a 112-electrode SuperSting R8 system (Advanced Geosciences, Inc.) with a 0.5 m electrode spacing, and a roll-along acquisition technique (Dafflon et al., 2016). Electrode locations were measured using a RTK differential GPS in 2011 and 2023. In 2023, the electrodes were placed along a measuring tape installed between control points every 50 meters that were either wooden poles remaining from the 2011 survey or re-surveyed based on the 2011 coordinates. While the RTK GPS-surveyed x–y coordinates were deemed precise enough for the goals of this study, the RTK-GPS elevation measurements contained some noise and inaccuracies associated with inconsistencies among the short surveys conducted over the three days of ERT acquisition, including in GPS signal quality, base station settings, and GPS pole positioning across organic-rich areas and in the presence of surface water. To increase accuracy, the elevation for each electrode was extracted from the DSMs, whose ground control targets were all surveyed consistently under ideal conditions

The collected ERT data used a dipole-dipole survey setup with a maximum distance of 18 meters between the nearest injection and potential electrodes and a maximum distance between adjacent injection (or potential) electrodes of 3 meters. Data quality control included the exclusion of low-quality measurements, including those with signal potentials below 3 mV. ERT datasets were processed and inverted using the open-source *pygimli* library and its *ERTManager* module (Rücker et al., 2017). A parameterized mesh was created for each campaign based on sensor positions, with mesh quality settings and electrode spacing tailored to improve resolution and reduce inversion artifacts. Differences between observed and modeled apparent resistivities were calculated to quantify model accuracy. For the 2011 dataset, a chi-squared value of 1.93 was achieved, along with an absolute mean percentage difference of 12.30% and a log-scale mean percentage difference of 2.41%.

https://doi.org/10.5194/egusphere-2025-2341
Preprint. Discussion started: 5 June 2025

The 2023 dataset achieved a chi-squared value of 1.94, an absolute mean percentage difference of 12.03%, and a log-scale mean percentage difference of 2.47%. Although the 2011 and 2023 surveys were both acquired in September, we note that differences in the ERT data need to be carefully interpreted given the inter-annual variability in climate forcing that impacts surface water distribution, thaw layer depth and moisture, as well as the slight differences in electrode positioning and topography that lead to different mesh grid for the inversion.

In addition, the thaw depth was measured at 3 m intervals along the ERT transect by pushing a tile probe in the ground until reaching frozen soil. Given these measurements were performed at the end of the warm season, we use these measurements as proxy for the active layer thickness (ALT) defined as the top layer of soil that thaws during the summer and refreezes in the winter in permafrost regions. The electrical resistivity of the ALT was estimated by averaging the resistivity values for mesh cells in the 0.5 m lateral interval around each measurement and from 0 to 0.5 m depth. Resistivity was also extracted from the 0.5 to 1 m and 1.0 to 1.5 m depth intervals using the same approach. The distribution of ALT, resistivity and topography were then visualized for each polygon type. Statistical significance of the differences across the polygon types was assessed using the Mann Whitney U test.

3 Results and Discussion

3.1 Spatio-temporal Variability in Microtopography and Surface Water Distribution

Our results indicate that decadal changes in topography and surface water are highly variable across the landscape, both in magnitude and distribution, with localized hotspots of permafrost degradation and surface water ponding (Fig. 1 and Fig. 2). Locations with significant increases in trough width and ponding are more noticeable in HCPs and FCPs than in LCPs. In the HCP area, a limited number of relatively large ponds formed in previously dry areas. By contrast, the increase in surface water in the FCP area is more evenly distributed, primarily associated with trough widening and small-scale variability in ground subsidence (Fig. 2). These fine-scale changes in the FCP area appear to contribute to an overall increase in surface water that is similar to or greater than that observed in the HCP area.

The observed increase in ponding along the transect aligns with the findings of Abolt et al. (2024), who estimated an average 11% annual net increase in thermokarst pool extent between 2010 and 2019 at a lowland site near Utqiaġvik (Abolt et al., 2024). While their study underlines that some ponds shrink while new ones form, our study does not indicate the presence of areas with significant decrease in surface water. However, it is important to note that the timing and frequency of data acquisition in our study are not ideally suited to detect possible decreases. Nonetheless, our results highlight varying modalities and extent of permafrost degradation across areas with different polygon topography.

https://doi.org/10.5194/egusphere-2025-2341
Preprint. Discussion started: 5 June 2025

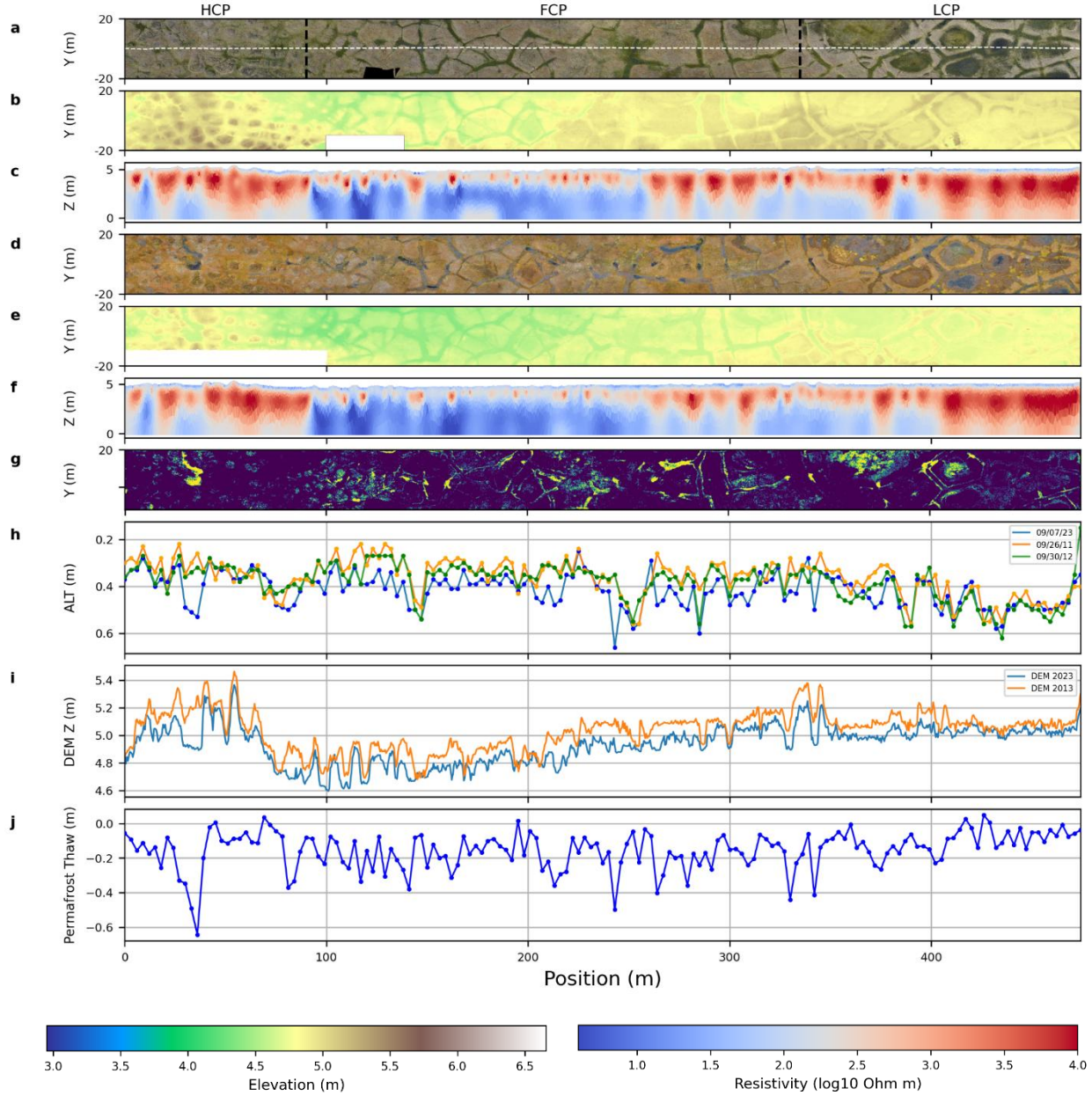

Figure 1. Surface and subsurface properties across various polygon types, including HCP (left), FCP (middle) and LCP (right). Datasets include a) 2013 RGB orthomosaic, b) 2013 ground elevation, c) 2011 ERT, d) 2023 RGB orthomosaic, e) 2023 ground elevation, f) 2023 ERT, g) pond expansion (in yellow) based on the RGB orthomosaics and a random forest algorithm, h) ALT measurements, i) elevation along the ERT transect, and j) estimated permafrost thaw based on changes in ALT and elevation. Note that in (g) the estimated pond expansions in the center of LCPs are artifacts.

https://doi.org/10.5194/egusphere-2025-2341
Preprint. Discussion started: 5 June 2025

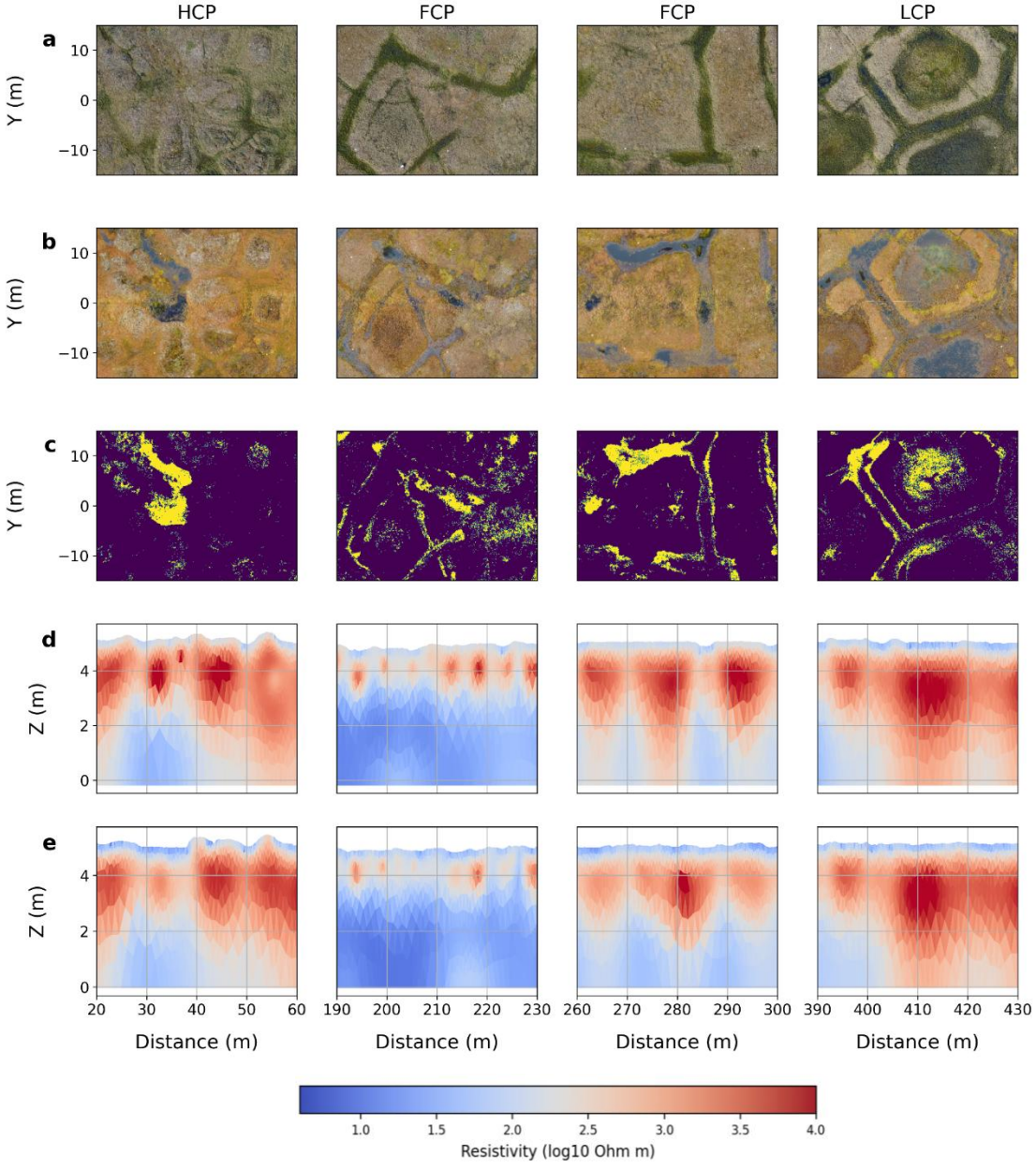

Figure 2. Decadal changes in surface and subsurface properties in four areas. Datasets include a) 2013 orthomosaic, b) 2023 orthomosaic, c) pond expansion (in yellow) based on the RGB orthomosaics and a random forest algorithm, d) 2011 ERT, and e) 2023 ERT. Note that the estimated pond expansions in the center of the LCP in (c) is an artifact.

https://doi.org/10.5194/egusphere-2025-2341
Preprint. Discussion started: 5 June 2025

3.2 Controls on Increased Surface Water, Thawing, and Subsidence

The observed decadal changes in surface water are accompanied by significant variations in ALT and resistivity, which differ by polygon type (Fig. 1). ALT increased significantly over the study period in FCP and HCP zones ($p < 0.05$), and increased below the threshold of significance in the LCP zone ($p = 0.083$) (Fig. 3). These changes are consistent with the observations of surface subsidence across the three zones, further supporting the interpretation of more intense permafrost thaw in HCPs and FCPs than in LCPs (Fig. 1 and Fig. 3).

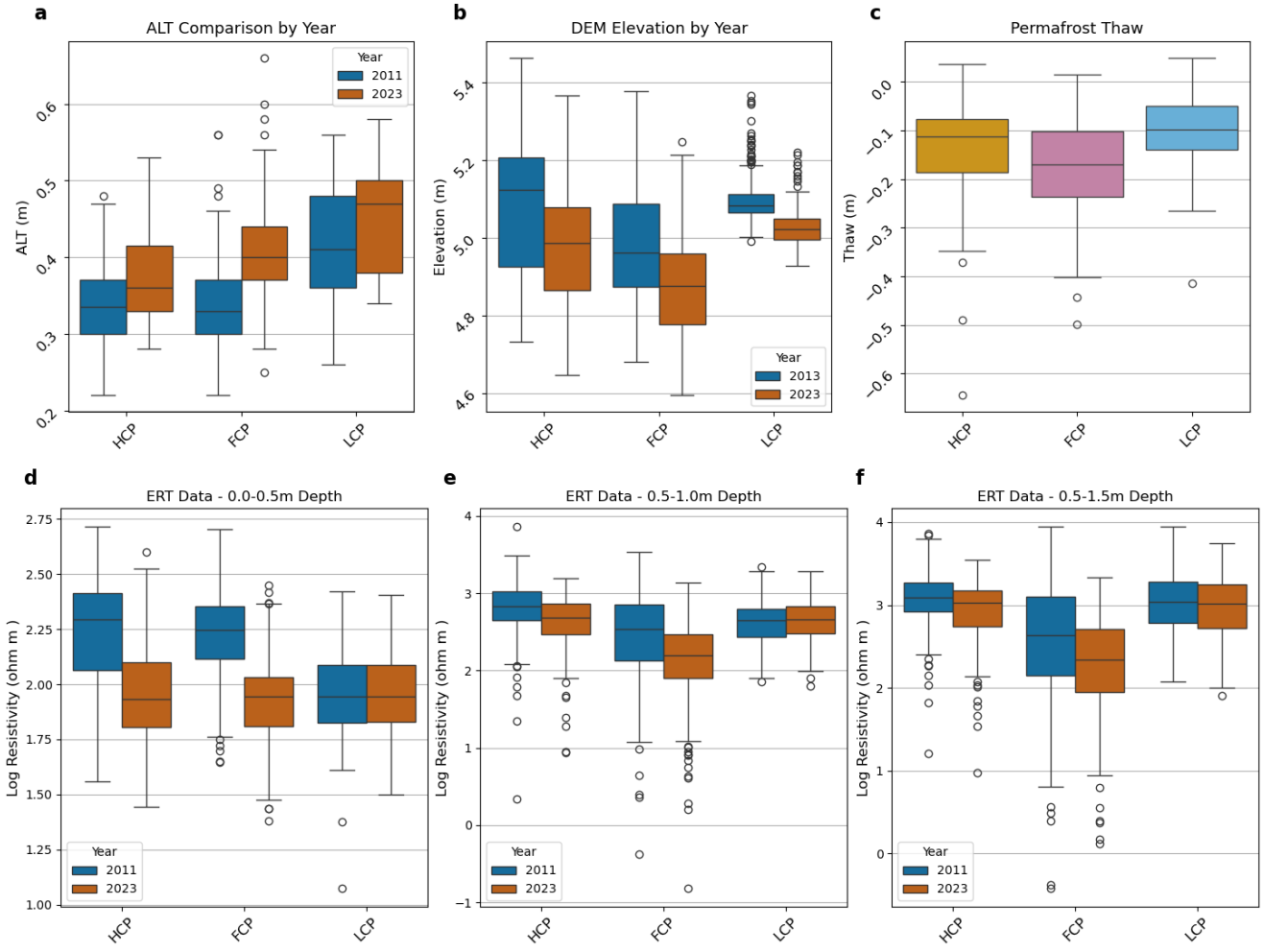

Figure 3. Evaluation by polygon types of changes in a) ALT, b) elevation, c) permafrost thaw, and average resistivity for the d) 0-0.5, e) 0.5-1 and f) 0.5-1.5 m depth interval. p-value for change between 2011 and 2023: a) HCP: 0.049, FCP: <0.001, LCP: 0.083 b) HCP: <0.001, FCP: <0.001, LCP: <0.001, d) HCP:<0.001, FCP: <0.001, LCP: 0.749, e) HCP: <0.001, FCP: <0.001, LCP: 0.316, and f) HCP: <0.001, FCP: <0.001, LCP: 0.315.

https://doi.org/10.5194/egusphere-2025-2341
Preprint. Discussion started: 5 June 2025

Electrical resistivity in the 0–0.5 m and 0.5–1 m depth intervals decreased significantly in both HCP and FCP areas ($p < 0.001$), consistent with a deepening of the active layer. This aligns with the expectation that, while the top organic layer may dry slightly during thaw, the overall volume of thawed material increases, with the lower portion of the thaw layer remaining wet due to ice melt and/or other hydrological processes (Dafflon et al., 2017; Rodenhizer et al., 2020; Tran et al., 2018). In contrast, no significant resistivity changes were observed in these depth intervals in the LCP area ($p > 0.3$), corroborating a slower rate of permafrost degradation.

Though HCP and FCP areas both show large increases in ALT, permafrost thaw, and water ponding, their spatial patterns of change are distinct due to different subsurface structures. ERT and soil core data from the site show that the HCP area is characterized by large troughs relative to polygon diameter, a large volume of ice wedges beneath the troughs, and numerous ice veins throughout the polygons (Fig. 1c). This ice presumably originates from freshwater and is therefore more resistive compared to surrounding saline material (Dafflon et al., 2016). Such zones with large troughs and ice content have been identified as more prone to further degradation (Kanevskiy et al., 2017). Indeed, the newly formed pond in the HCP area observed in Figure 2 shows surface characteristics similar to those reported at a different site (Figures S12–S16 in Kanevskiy et al., 2017). Although the exact conditions that led to pond formation are unknown, Kanevskiy et al. (2017) reported that these features are typically triggered by an increase in ALT during exceptionally warm and wet summers. Additionally, a snow survey across various polygon types at a nearby site found that HCPs are associated with much higher spatial variability in snow depth than FCPs or LCPs (Wainwright et al., 2017), which could participate to the particularly heterogeneous subsidence observed in the HCP area.

In contrast with the HCP area, the FCP area exhibits ice-rich permafrost limited to shallow depths, a strong salinity gradient with depth, and the presence of relatively small ice wedges beneath the troughs (Fig. 1c) (Dafflon et al., 2016). The smaller amount of ice in FCP compared to HCP or LCP areas may contribute to faster degradation as less latent heat must be absorbed. The relatively low amount and heterogeneity of ice-content in this area are also expected to constrain the magnitude and variability of subsidence. Our observations of subsidence, along with the fact that the topography is relatively flat, align closely with this conceptual model. The FCP area shows relatively even subsidence across the zone, with small changes occurring at many locations, including in trough, rim and center.

Finally, the LCP area shows less significant increases in ALT, degradation, or subsidence. LCPs tend to have a large amount of surface water, and geophysical and soil core data tend to show that the LCP area has a greater ice-content than the FCP. While their ice-content is more similar to HCP, the permafrost structure is more ataxitic with a lower presence of ice veins and ice wedges (Fig. 1c and Fig. 2) (Dafflon et al., 2016). The LCP landscape and subsurface structure appear to contribute to more stable conditions during the period of this study.

Overall, while this study does not attempt to fully disentangle the effects of surface water (dominant in LCPs), microtopography-driven snow distribution, and the role of ice-rich material on latent heat and subsidence, the results demonstrate that subsidence occurs with varied patterns across the landscape, including varying intensity and unevenness. Spatially variable subsurface characteristics and thaw rates are key drivers of the amount and distribution of subsidence. In

https://doi.org/10.5194/egusphere-2025-2341
Preprint. Discussion started: 5 June 2025

addition, the results of this study reinforce the conclusion of Kanevskiy et al. (2017) that understanding the contrast between degradation and stability across areas, and the associated evolution of the landscape, remains complex.

3.3 Challenges in Capturing Variability in Thermal and Hydrological Trajectories

The results of this study highlight the value of collecting independent datasets that capture above-ground, ground-surface, and subsurface properties to gain a comprehensive understanding of hydrological changes in permafrost systems. Multiple datasets are needed due to the complexity of geomorphological and hydrological changes occurring during permafrost degradation, as well as the uncertainties inherent in individual measurements, which may lead to misinterpretation when considered independently. For example, integrating thaw thickness measurements with ground elevation changes for estimating permafrost degradation is crucial to avoid the underestimation of thaw rates, ice volume loss, and soil mass loss (Rodenhizer et al., 2020). In the present study, where decadal changes in thaw depth are expected to be limited compared to lower latitudes where both permafrost and air temperatures are warmer, measuring variation in topography has still proven to be important for capturing small changes that may accelerate as ice melts. Subsidence is consistent with variations in thaw depth when averaged across the various polygon types, but they are not strongly correlated across each individual point due to the heterogeneity of ice content and thaw rates. Overall, the convolution of spatially varying thaw rates and ice content creates large heterogeneity in hydrological and topographic changes.

Capturing fine-scale elevation and its temporal changes in Arctic permafrost environments poses significant challenges, particularly concerning uncertainty and accuracy. In-field assessment of ground surface elevation is complicated by the presence of a soft organic layer with highly variable water content and a poorly defined transition between the peat layer and vegetation (e.g., dwarf shrubs, graminoids, and mosses). The presence of surface water poses an additional challenge, and these factors together give rise to considerable uncertainty in locating ground-based measurements, which typically use the ground surface as a reference point. An additional source of uncertainty in ground elevation between repeated surveys is coordinate system alignment and correction. These uncertainties are especially critical in contexts like this study, where small spatial and temporal variations in ground surface elevation have a major impact on surface and subsurface hydrology. Overall, ground elevation and its associated uncertainty affect many data products, including subsidence estimates, permafrost thaw characterization, topographic metrics (e.g., surface flow lines), and the comparability of time-lapse ERT datasets. In high-resolution ERT surveys, accounting for topographic variation complicates data comparison over time due to differences in surface conditions, inversion meshes, and the associated regularization and convergence processes.

The above-mentioned complexity underscores the importance of developing strategies to manage uncertainties as effectively as possible, and bridging temporal and spatial scales in coverage and resolution. While sporadic above- and below-ground surveys such as those conducted here are valuable for model evaluation and satellite data product development, their interpretation requires careful consideration of seasonal and interannual variability, as well as the limited spatial coverage that constrains their representativeness across the Arctic. Our study draws on datasets from years that align relatively closely,

https://doi.org/10.5194/egusphere-2025-2341
Preprint. Discussion started: 5 June 2025

though with slightly higher active layer thickness, with the long-term fitted trend at the nearby CALM site (Fig. S1). Results may differ in an exceptionally warm or cold year. Improving the temporal resolution and associated understanding in subsurface variables, such as using CALM or other monitoring networks data, is becoming increasingly feasible due to the growing availability and affordability of autonomous instrumentation (Dafflon et al., 2017; Fiolleau et al., 2024), as well as community efforts in discussing best practices in data acquisition, including for ERT (Herring et al., 2023). Further, due to increase in resolution, satellite imagery may become well-suited for integration with ground-based data to facilitate scaling while possibly better capturing changes in shallow surface water distribution with more surveys conducted under similar conditions of water color, turbidity, and vegetation cover (Abolt et al., 2024). The results of this study advocate for further integration of multiple datasets across a range of scales to improve the understanding of controls on water ponding formation and drying, assess permafrost thaw and ice melt, and disentangle the impact of thawing mechanisms on water distribution from changes in lateral inputs caused by rerouted surface flow.

4 Conclusions

This study documents changes occurring within polygonal tundra landscapes over a decadal timescale in Utqiaġvik, Alaska. Our findings demonstrate that changes in surface water distribution are closely linked to subsidence, increased permafrost thaw, and decreased permafrost resistivity. Additionally, more intense thaw and ice loss is observed in HCPs and FCPs than in LCPs. The localized and complex increases in thermokarst ponding and trough widening observed at the study site underscore the importance of combining multiple data products to capture the intensity and spatial heterogeneity of subsidence and its controls. The results also support the need for future studies that can better characterize the small- and medium-scale feedback mechanisms associated with permafrost thaw. Such insights are essential for refining models that simulate Arctic ecosystem responses to a warming climate, ultimately improving our understanding of how permafrost thaw contributes to changes in global carbon cycling.

Data availability

The 2023 survey, 2011 ERT, and 2013 UAV datasets presented in this study have been submitted to the ESS-DIVE repository at https://data.ess-dive.lbl.gov/datasets/doi:10.15485/2564382, https://data.ess-dive.lbl.gov/datasets/doi:10.5440/1233229, and https://data.ess-dive.lbl.gov/datasets/doi:10.5440/1177858, respectively.

Author contributions

BD, CU and JL planned this study and collected the various datasets in 2011, 2013, and 2023. JB and BD analyzed the datasets and prepared the manuscript. JL and NT reviewed the manuscript. All authors contributed to the study and approved the final version of the paper.

https://doi.org/10.5194/egusphere-2025-2341
Preprint. Discussion started: 5 June 2025

Competing interests

The authors declare that they have no conflict of interest.

Acknowledgments

We thank UIC Science for their guidance and for allowing us to conduct our research on the traditional homelands of the Iñupiat. We thank the CALM program and community for making data publicly available. The authors also thank NOAA Barrow Atmospheric Baseline Observatory for the atmospheric data used in this study. We thank Robin Thibault for support on using *pygimli* library. This material is based upon work supported by Next-Generation Ecosystem Experiments (NGEE Arctic) funded by the U.S. Department of Energy Office of Science Office of Biological and Environmental Research (award no. DE-AC02-05CH11231).

Financial Support

The Next Generation Ecosystem Experiment (NGEE) Arctic project is supported by the Office of Biological and Environmental Research in the U.S. Department of Energy's Office of Science (award no. DE-AC02-05CH11231).

References

Abolt, C. J., Atchley, A. L., Harp, D. R., Jorgenson, M. T., Witharana, C., Bolton, W. R., Schwenk, J., Rettelbach, T., Grosse, G., Boike, J., Nitze, I., Liljedahl, A. K., Rumpca, C. T., Wilson, C. J., & Bennett, K. E. (2024). Topography controls variability in circumpolar permafrost thaw pond expansion. *Journal of Geophysical Research. Earth Surface*, *129*(9), e2024JF007675.

Brown, J. (1969). Ionic concentration gradients in permafrost, Barrow, Alaska. *Cold Regions Research and Engineering Laboratory (U.S.), Research Report 272*.

Dafflon, B., Hubbard, S., Ulrich, C., Peterson, J., Wu, Y., Wainwright, H., & Kneafsey, T. J. (2016). Geophysical estimation of shallow permafrost distribution and properties in an ice-wedge polygon-dominated Arctic tundra region. *Geophysics*, *81*(1), WA247–WA263.

Dafflon, B., Oktem, R., Peterson, J., Ulrich, C., Tran, A. P., Romanovsky, V., & Hubbard, S. S. (2017). Coincident aboveground and belowground autonomous monitoring to quantify covariability in permafrost, soil, and vegetation properties in Arctic tundra. *Journal of Geophysical Research: Biogeosciences*. https://doi.org/10.1002/2016jg003724

Farquharson, L. M., Romanovsky, V. E., Kholodov, A., & Nicolsky, D. (2022). Sub-aerial talik formation observed across the discontinuous permafrost zone of Alaska. *Nature Geoscience*, *15*(6), 475–481.

Fiolleau, S., Uhlemann, S., Shirley, I. A., Wang, C., Wielandt, S., Rowland, J., & Dafflon, B. (2024). Insights on seasonal solifluction processes in warm permafrost Arctic landscape using a dense monitoring approach across adjacent hillslopes. *Environmental Research Letters*. https://doi.org/10.1088/1748-9326/ad28dc

Herring, T., Lewkowicz, A. G., Hauck, C., Hilbich, C., Mollaret, C., Oldenborger, G. A., Uhlemann, S., Farzamian, M., Calmels, F., & Scandroglio, R. (2023). Best practices for using electrical resistivity tomography to investigate permafrost. *Permafrost and Periglacial Processes*, *34*(4), 494–512.

Hinkel, K. M., Doolittle, J. A., Bockheim, J. G., Nelson, F. E., Paetzold, R., Kimble, J. M., & Travis, R. (2001). Detection of subsurface permafrost features with ground-penetrating radar, Barrow, Alaska. *Permafrost and Periglacial Processes*, *12*(2), 179–190.

https://doi.org/10.5194/egusphere-2025-2341
Preprint. Discussion started: 5 June 2025

Jorgenson, M. T., Shur, Y. L., & Pullman, E. R. (2006). Abrupt increase in permafrost degradation in Arctic Alaska. *Geophysical Research Letters*, *33*(2). https://doi.org/L02503 10.1029/2005gl024960

Kanevskiy, M., Shur, Y., Jorgenson, T., Brown, D. R. N., Moskalenko, N., Brown, J., Walker, D. A., Raynolds, M. K., & Buchhorn, M. (2017). Degradation and stabilization of ice wedges: Implications for assessing risk of thermokarst in northern Alaska. *Geomorphology (Amsterdam, Netherlands)*, *297*, 20–42.

Kokelj, S. V., & Jorgenson, M. T. (2013). Advances in thermokarst research. *Permafrost and Periglacial Processes*, *24*(2), 108–119.

Koven, C. D., Ringeval, B., Friedlingstein, P., Ciais, P., Cadule, P., Khvorostyanov, D., Krinner, G., & Tarnocai, C. (2011). Permafrost carbon-climate feedbacks accelerate global warming. *Proceedings of the National Academy of Sciences of the United States of America*, *108*(36), 14769–14774.

Mackay, J. R. (2000). Thermally induced movements in ice-wedge polygons, western Arctic coast: A long-term study. *Geographie Physique Et Quaternaire*, *54*(1), 41–68.

Rodenhizer, H., Ledman, J., Mauritz, M., Natali, S. M., Pegoraro, E., Plaza, C., Romano, E., Schädel, C., Taylor, M., & Schuur, E. (2020). Carbon Thaw Rate Doubles When Accounting for Subsidence in a Permafrost Warming Experiment. *Journal of Geophysical Research: Biogeosciences*, *125*(6), e2019JG005528.

Rücker, C., Günther, T., & Wagner, F. M. (2017). pyGIMLi: An open-source library for modelling and inversion in geophysics. *Computers & Geosciences*, *109*(Supplement C), 106–123.

Shiklomanov, N. (2023). *Thaw depth measurements from the Circumpolar Active Layer Monitoring (CALM) project for site "Barrow, CRREL Plots" (U2), Alaska North Slope, United States, Alaska (1962-2023)*. Arctic Data Center, doi:10.18739/A27940W32.

Shiklomanov, N. I., Streletskiy, D. A., Little, J. D., & Nelson, F. E. (2013). Isotropic thaw subsidence in undisturbed permafrost landscapes. *Geophysical Research Letters*, *40*(24), 6356–6361.

Streletskiy, D. A., Shiklomanov, N. I., Little, J. D., Nelson, F. E., Brown, J., Nyland, K. E., & Klene, A. E. (2017). Thaw subsidence in undisturbed tundra landscapes, barrow, Alaska, 1962-2015. *Permafrost and Periglacial Processes*, *28*(3), 566–572.

Tarnocai, C., Canadell, J. G., Schuur, E. A. G., Kuhry, P., Mazhitova, G., & Zimov, S. (2009). Soil organic carbon pools in the northern circumpolar permafrost region. *Global Biogeochemical Cycles*, *23*. https://doi.org/Gb2023 10.1029/2008gb003327

Tran, A. P., Dafflon, B., Bisht, G., & Hubbard, S. S. (2018). Spatial and temporal variations of thaw layer thickness and its controlling factors identified using time-lapse electrical resistivity tomography and hydro-thermal modeling. *Journal of Hydrology*, *561*, 751–763.

Wainwright, H. M., Liljedahl, A. K., Dafflon, B., Ulrich, C., Peterson, J. E., Gusmeroli, A., & Hubbard, S. S. (2017). Mapping snow depth within a tundra ecosystem using multiscale observations and Bayesian methods. *The Cryosphere*, *11*(2), 857–875.

Wu, Y., Ulrich, C., Kneafsey, T., Lopez, R., Chou, C., Geller, J., McKnight, K., Dafflon, B., Soom, F., Peterson, J., & Hubbard, S. S. (2018). Depth-Resolved Physicochemical Characteristics of Active Layer and Permafrost Soils in an Arctic Polygonal Tundra Region. *Journal of Geophysical Research: Biogeosciences*, *123*(4), 1366–1386.